Indian Journal of Geo Marine Sciences
Vol. 48 (06), June 2019, pp. 952-956

Sharp-edged orifice plate's wall pressure characteristics

Wanzheng Ai[1*] & Tianming Ding[2]

[1,2]Zhejiang Ocean University, Zhoushan City 316021, China, Associate Professor

[*][E-mail: aiwanzheng@126.com]

Received 11 July 2016; revised 28 November 2016

The minimum wall pressure coefficient of orifice plate and its wall pressure distribution relating to tunnel's and dissipater's safety are important indices for this energy dissipater design. In the present paper, the minimum wall pressure coefficient of sharp-edged orifice plate was analyzed; meanwhile, the characteristics of sharp-edged orifice plate wall pressure distribution were also analyzed. The research result has shown that the minimum wall pressure coefficient was mainly dominated by the contraction ratio of the orifice plate. The less is the contraction ratio of the orifice plate, the larger is the minimum wall pressure coefficient. The effect of orifice plate' thickness on the minimum wall pressure coefficient was not obvious and could be neglected. When Reynolds number is more than 10^5, it has little impact on the minimum wall pressure coefficient. Wall pressure begins to drop down dramatically before 0.5*D* orifice plate, reaches minimum at the end of orifice plate, and then recovers normally when flows arrival at 3*D* away after orifice plate. An empirical expression was presented to calculate the minimum wall pressure coefficient. Experimental data illuminate that calculation results by using empirical expression coincided with experiment results.

[Keywords: Orifice plate; Wall pressure, Minimum wall pressure coefficient; Contraction ratio; Reynolds number]

Introduction

With the development of hydropower projects, the heights of some dams exceed the level of 300 m, for example 305 m and 315 m for the Jinping first-cascade hydropower project and the Shuangjiangkou hydropower project in Sichuan province, China, respectively. Over 30 hydropower projects with the height of over 100 m have been completed or are under construction since 2000, in China. For any high dam project, the energy dissipation for flood discharges is an important problem that affects the safety of the project directly[1]. The orifice plate as well as the plug, as a kind of energy dissipaters with sudden reduction and sudden enlargement forms, has been used in the hydropower projects due to its simple structure, convenient construction and high energy dissipation ratio. As early as 1960s in the last century, a plug dissipater, similar to orifice plate in energy dissipation mechanism, with the energy dissipation ratio of over 50%, was used in the flood discharge tunnel of the Mica dam in Canada[2] In 2000, a three-stage orifice plate was applied in the Xiaolangdi projects in china, gets the energy dissipation ratio of about 44% and effectively controlled the flow velocity through the gate less than 35 m/s under the condition of the head of 145 m[3].

Many studies have been conducted on the orifice plate, in which the energy dissipation and the cavitation are the two main items. Orifice plate's energy dissipation characteristics and its cavitation characteristics are mainly dominated by its contraction ratio, which is defined as the ratio of the orifice diameter (*d*) of the energy dissipater and the diameter (*D*) of flood discharge tunnel. Jianhua[4] deemed that orifice plate's energy loss coefficient, embodying orifice plate's energy dissipation capacity, decreases with the increase of contraction ratio. Cavitation performance has been another important item of the orifice plate and could be characterized by its incipient cavitation number. Bullen[5] and Shanjun[6] regarded that the incipient cavitation number of the orifice plate decreased with the increase of the contraction ratio. As stated above, the researches conducted in the past focused mainly on energy loss coefficient and incipient cavitation number[7,9]. As a matter of fact, many other coefficients, such as orifice plate's minimum wall pressure coefficient also have important effects on orifice plate design. Because the position of cavitations first happening often locates at the point where the minimum pressure occurs in the

vicinity of orifice plate, the minimum wall pressure coefficient of the orifice plate can more directly reflect the tunnel wall's capacity of resisting cavitation damage[10]. Unfortunately, there is less research on orifice plate minimum wall pressure coefficient. The purpose of the present work was to investigate the effects of the geometric parameters, i.e., contraction ratio and hydraulic parameters on the minimum wall pressure coefficient when orifice plate's top angle φ is 60^0 and also to present empirical expression of the minimum wall pressure coefficient, by means of numerical simulations (Fig. 1).

Numerical Simulations

Numerical simulations model

The RNG k∼ε model was used to calculate the hydraulic parameters of the flow through the orifice plate, due to its suitability for simulating the flow inside large change boundary forms as well as its high precision and calculation stability[11]. For the steady and incompressible flows, the governing equations of this model can be written as[12,13]:

Continuity equation:

$$\frac{\partial u_i}{\partial x_i} = 0 \quad i = 1, 2 \qquad \ldots (1)$$

Momentum equation:

$$u_j \frac{\partial u_i}{\partial x_j} = -\frac{1}{\rho}\frac{\partial p}{\partial x_i} + \frac{\partial}{\partial x_j}[(\nu + \nu_t)(\frac{\partial u_i}{\partial x_j} + \frac{\partial u_j}{\partial x_i})] \quad i = 1, 2 \ldots (2)$$

k–equation:

$$u_i \frac{\partial k}{\partial x_i} = \frac{\partial}{\partial x_j}\left[\alpha_k (\nu + \nu_t)\frac{\partial k}{\partial x_j}\right] + \frac{1}{\rho}G_k - \varepsilon \quad i = 1, 2 \quad \ldots (3)$$

ε–equation:

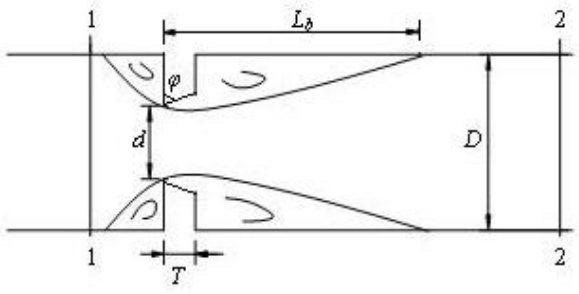

Fig. 1 — Flow through sharp-edged orifice plate

$$u_i \frac{\partial \varepsilon}{\partial x_i} = \frac{\partial}{\partial x_j}\left[\alpha_\varepsilon (\nu + \nu_t)\frac{\partial \varepsilon}{\partial x_j}\right] + \frac{1}{\rho}C_1^* G_k \frac{\varepsilon}{k} - C_2 \frac{\varepsilon^2}{k} \quad i = 1, 2 \ldots (4)$$

where x_i (= x, y) are the coordinates in longitudinal and transverse directions, respectively; u_i (= u_x, u_y) are the velocity components in x and y directions, respectively; ρ is the density of water; p is the pressure; v is the kinematics viscosity; v_t is the eddy viscosity and can be given by $v_t = C_\mu(k^2/\varepsilon)$, in which k is the turbulence kinetic energy, ε is the dissipation rate of k and $C_\mu = 0.085$. The other parameters are[14]: $C_1^* = C_1 - \frac{\eta(1-\eta/\eta_0)}{1+\lambda\eta^3}$, $\eta = Sk/\varepsilon$, $S = \frac{1}{2}\left(\frac{\partial u_i}{\partial x_j} + \frac{\partial u_j}{\partial x_i}\right)$, C_1 =1.42, $\eta_o = 4.377$, $\lambda = 0.012$, $G_k = \rho\nu_t\left(\frac{\partial u_i}{\partial x_j} + \frac{\partial u_j}{\partial x_i}\right)\frac{\partial u_i}{\partial x_j}$, C_2 =1.68 and $\alpha_k = \alpha_\varepsilon = 1.39$. The calculation boundary conditions are treated as follows: in the inflow boundary the turbulent kinetic energy k_{in} and the turbulent dissipation rate ε_{in} can be defined as respectively[14]:

$$k_{in} = 0.0144u_{in}^2, \quad \varepsilon_{in} = k_{in}^{1.5}/(0.25D) \qquad \ldots (5)$$

where u_{in} is the average velocity in the inflow boundary. In the outflow boundary, the flow is considered as developed fully. The wall boundary is controlled by the wall functions[15]. And the symmetric boundary condition is adopted, that is, the radial velocity on symmetry axis is zero.

Numerical simulations methodology

Because the orifice plate tunnel has axial symmetry characteristics, three-dimensional(3-D) numerical simulations of orifice plate tunnel flows can be simplified as two-dimensional(2-D) numerical simulations of orifice plate tunnel flows. The 3-D coordinate axis of orifice plate tunnel is shown in Figure 2. In this paper, flows' characteristics of plane XZ are researched; the characteristics of flows in plane XZ can represent the whole orifice plate tunnel flows characteristics.

The minimum wall pressure coefficient is defined as:

$$c_p = \frac{p_0 - p_{\min}}{0.5\rho u^2} \qquad \ldots (6)$$

where p_0 is the average pressure at undisturbed section before orifice plate, the undisturbed section

can be regarded at or before 3*D* orifice plate location; c_p is the minimum wall pressure coefficient; p_{min} is the lowest wall pressure; ρ is water's density; and u is the average flow velocity in tunnel. Because cavitations in the vicinity of wall first happen at the lowest pressure place, the less is the p_{min}, the larger is the chance of happening cavitation. The minimum wall pressure coefficient of orifice plate can demonstrate orifice plate's cavitations characteristics, the less is the minimum wall pressure coefficient, the better is the ability of orifice plate resisting cavitations damage.

There are many parameters which affect the minimum wall pressure coefficient of orifice plate. The relevant parameters of dimensional analysis may include: Density of water ρ (kg/m^3); dynamic viscosity of water μ (N.s/m^2); tunnel diameter D (m); orifice plate diameter d; orifice plate thickness T (m); average flow velocity in tunnel u (m/s), and difference between p_0 and p_{min} (p_0 - p_{min}) (Pa). Because each of the above parameters is a function of the initial independent parameters, the expression about the above parameters can be obtained:

$$p_0 - p_{min} = f(D, d, T, \rho, \mu, u) \quad \ldots (7)$$

This relationship could be rewritten in terms of dimensionless parameters:

$$(p_0 - p_{min})/(0.5\rho u^2) = f(d/D, T/D, uD\rho/\mu) \quad .. (8)$$

That is:

$$c_p = f(d/D, T/D, Re) \quad \ldots (9)$$

where Re is Reynolds number, $Re=uD\rho/\mu$. Eq. (9) indicates that the minimum wall pressure coefficient of orifice plate c_p is the function of d/D, T/D, Re.

According to Eq. (9), two kinds of calculation phases were simulated: Phase No. 1 calculates the minimum wall pressure coefficient of orifice plate c_p at the range of Reynolds number Re= 9.00×10^4 – 2.76×10^6 when d/D = 0.50 and T/D = 0.10, to analyze the effects of Re on c_p and Phase No. 2 that calculates c_p at the different d/D and T/D when Re = 1.80×10^5, to discuss the variations of c_p with d/D and T/D. The calculation operation pressure in the inflow boundary is a standard atmospheric pressure. The inflow boundary is located before 3*D* orifice plate, the outflow boundary is located after 6*D* orifice plate.

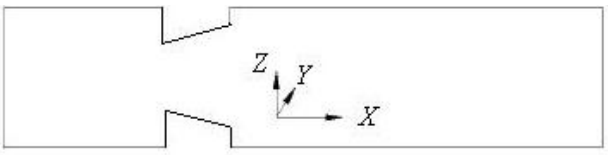

Fig. 2 — 3-D coordinate axis of orifice plate tunnel

Results and Discussion

The simulation results of Phase No.1 are shown in Table 1, where, the pressures are neglect values; this is because the calculation operation pressure in the inflow boundary is designed as a standard atmospheric pressure. It can be concluded from Table 1 that when Reynolds number Re is less than 10^5, c_p increases slightly with the increase of Reynolds number Re, but when Reynolds number Re is more than 10^5, Reynolds number Re has no impact on Re and its effects can be neglected.

The results of Phase No. 2 are shown in Table 2. It can be learnt that relative thickness T/D has little effect on c_p, i.e. when the contraction ration d/D is 0.5, relative thickness T/D varies from 0.05 to 0.25 and c_p approximately remains stable at 56. Table 2 also demonstrates that c_p is mainly dominated by contraction ratio d/D. If the effects of Reynolds number and relative thickness T/D on c_p are neglected, the relationships between c_p and d/D are shown in Figure 3, which is drawn by using the data in Table 2 when T/D is 0.1. The following formula can be obtained by fitting the curve in Figure 3:

$$c_p = -4273.3(d/D)^3 + 8995.5(d/D)^2 - 6351.1(d/D) + 1519.1 \quad \ldots (10)$$

This expression is valid for d/D= 0.4 – 0.8, $Re > 10^5$, and the effects of T/D on c_p being neglected.

Model Experiment

Model arrangement

The physical model experimental set-up consists of an intake system, a tank, a flood discharge tunnel with

Table 1 — The calculation results of Phase No.1 (d/D = 0.50 and T/D = 0.10)

Re ($\times10^5$)	0.90	1.80	9.20	18.40	27.60
P_0(p_a)	-10.12	-28.01	-581.43	-630.12	-3252.28
p_{min}(p_a)	-6491.58	-27961.99	-698795.41	-2796877.01	-6291139
c_p	54.38	55.98	55.98	55.98	55.98

Table 2 — The calculation results of Phase No.2 ($Re = 1.80\times10^5$)

d/D	parameter	T/D 0.05	0.10	0.15	0.20	0.25
	P_0(pa)	/	-19.01	/	/	/
0.40	p_{min}(pa)	/	-72427.81	/	/	/
	c_p	/	144.89	/	/	/
	P_0(pa)	-28.09	-27.01	-28.98	-27.54	-28.01
0.50	p_{min}(pa)	-28336.91	-28288.73	-28281.02	-28272.46	-27961.99
	c_p	56.73	56.63	56.62	56.60	55.98
	P_0(pa)	-33.01	-33.01	-34.12	-34.01	-34.98
0.60	p_{min}(pa)	-13126.99	-13109.45	-13100.88	-13090.99	-13070.02
	c_p	26.32	26.29	26.27	26.25	26.21
	P_0(pa)	/	-40.00	/	/	/
0.70	p_{min}(pa)	/	-6827.98	/	/	/
	c_p	/	13.74	/	/	/
	P_0(pa)	/	-47.01	/	/	/
0.80	p_{min}(pa)	/	-3867.56	/	/	/
	c_p	/	7.83	/	/	/

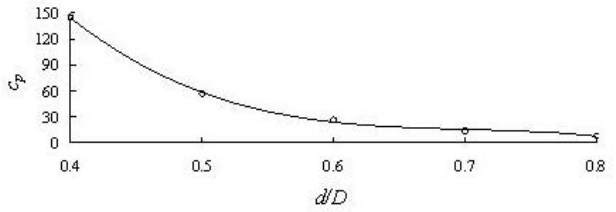

Fig. 3 — The relationships between c_p and *d/Ds*

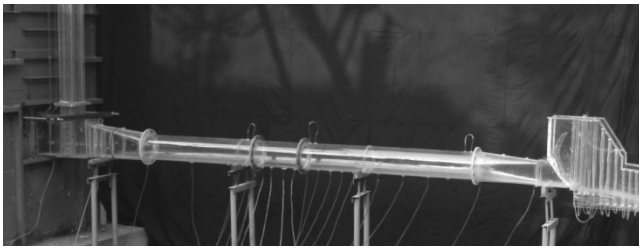

Fig. 4 — The discharge tunnel model

an orifice plate energy dissipater, and a return system with a rectangular weir (Fig. 3). The diameter (*D*) of the tunnel model is 0.21 m and the length of the tunnel model is 4.75 m, i.e., 22.6 *D* from the intake to the pressure tunnel outlet at the gate. The orifice plate energy dissipater was placed at the positions of 10.0 *D* from the tunnel intake and of 12.6 *D* away from the outlet at the gate. The water head about 10.0 *D* could be presented by the intake system and the tank. The opening of the gate could be changed conveniently. The discharge tunnel model is shown in Figure 4.

Analysis for results

Table 3 gives comparison results between experimented data and calculation results obtained by using Eq. (10). The symbols in Table 3 are explained as: $c_{p.eq}$ is the minimum wall pressure coefficient by calculation using Eq. (10), $c_{p.ex}$ is experiment minimum wall pressure coefficient, and E_r is the comparison result between $c_{p.eq}$ and $c_{p.ex}$. which can be expressed as:

Table 3 — comparison results between experiment data and calculation results

d/D	$c_{p.ex}$	$c_{p.eq}$	E_r (%)
0.690	15.6	15.8	1.3
0.755	10.8	12.6	13.6
0.800	7.5	7.4	1.4

$$E_r = \frac{\left|c_{p.eq} - c_{p.ex}\right|}{c_{p.ex}} \times 100\% \quad \ldots (11)$$

The results in Table 3 illuminate that the calculation results obtained by using Eq. (10) coincided with experiment results and the relative errors of Eq. (10) are all less than 13.6%.

Conclusion

For sharp-edged orifice plate, its minimum wall pressure coefficient c_p is the function of the contraction ratio *d/D*, relative thickness *T/D*, and Reynolds number *Re*. The effects of orifice plate' thickness on the minimum wall pressure coefficient was not obvious and therefore could be neglected. When Reynolds number is more than 10^5, it little impact on the minimum wall pressure coefficient.

The contraction ratio *d/D* is the key factor that dominates the minimum wall pressure coefficient c_p.

The minimum wall pressure coefficient c_p decreases with the increase of contraction ratio. The relationship of c_p and d/D could be expressed as Eq. (10). Comparing the calculation results and the physical model experimental results, the relative errors of Eq. (10) are all less than 13.6 %.

Acknowledgement

The paper was supported by the CRSRI Open Research Program, Ningxia higher educational scientific research projects(Grant No. NGY2018-241) and National Natural Science Foundation of China.

References

1 Tong, X., Junmei, C. Study and practice of interior energy dissipater for flood discharge tunnels. *Journal of Water Conservancy and Hydropower Technology,*30(12) (1999), 69–71. (in Chinese)

2 Russel, S.O., Ball, J.W. Sudden- enlargement energy dissipater for Mica dam. *Journal of the Hydraulics Division*, ASCE**,** 93(4), (1967)41-56.

3 Wanzheng, A., Qi, Z. Hydraulic characteristics of multi-stage orifice plate. *Journal of Shanghai Jiaotong University* (science), 19(3), (2014)361-366.

4 Jianhua, W., Wanzheng, A. Head loss coefficient of orifice plate energy dissipaters. *Journal of hydraulic research,* 48(4), (2010) 526-530.

5 Bullen, P.R., Cheeseman, D.J., Hussain, L.A., Ruffellt, A.E. The determination of pipe contraction pressure loss coefficients for incompressible turbulent flow. *Journal of Heat and Fluid Flow*, 8(2), (1987)111-118.

6 Shanjun, L., Yongquan, Y., Weilin, X., Wei, W. Hydraulic characteristics of throat-type energy dissipater in discharge tunnel. *Journal of Hydraulic Engineering,* 7(2002) 42-52. (in Chinese)

7 Huiqin, Z. Discussion on multi-orifice plate energy dissipation coefficient. *Journal of Water Conservancy and Hydropower Technology,* 6(1993) 45-50. (in Chinese)

8 Qingfu, X., Hangen, N. Numerical simulation of plug energy dissipater. *Journal of Hydraulic Engineering,* 8(2003) 37-42. (in Chinese) (in Chinese)

9 Jianhua, W., Wanzheng, A. Flows through energy dissipaters with sudden reduction and sudden enlargement forms. *Journal of hydrodynamics, Ser.B*, 22(3), (2010)234-343.

10 Wanzheng, A., Jianhua, W. Comparison on hydraulic characteristics between orifice plate and plug .*Journal of Shanghai Jiaotong University* (science), 19(4), (2014)476-480.

11 ChangBing, Z., Yongquan, Y. 3-D numerical simulation of flow through an orifice spill way tunnel. *Journal of hydrodynamics,* Ser. B, 3(2002)83-90.

12 Yongquan, Y., Haiheng, Z. Numerical simulation of turbulent flows passed through an orifice energy dissipator within a flood discharge tunnel. *Journal of Hydrodynamics, Ser.B*, 4(3), (1992)27-33.

13 Hua, Z. Numerical analysis of the 3-D flow field of pressure atomizers with V-shaped cut at orifice. *Journal of hydrodynamics, Ser.B*, 23(2), (2011)187-192.

14 Zhong, T., Weilin, X., Shanjun, L., Wei, W., Jianmin, Z., Hui, D. Numerical simulation of composite plug energy dissipater. *Advances in Science and Technology of Water Resources,* 25(3), (2005)8-10. (in Chinese)